Improve mechanical properties of high pressure die cast Al9Si3Cu alloy via dislocation enhanced precipitation

Yijie Zhang*, Shihao Wang, Ewan Lordan, Yun Wang, Zhongyun Fan

Brunel Centre for Advanced Solidification Technology (BCAST), Brunel University London, Kingston Lane, Uxbridge UB8 3PH, United Kingdom

*Corresponding author. Tel.: +441895268538; Fax: +441895269758; E-mail address: yijie.zhang@brunel.ac.uk.

Abstract

To improve the properties of high pressure die cast Al9Si3Cu alloy, melt treatment via high shear was employed to form fine in-situ $MgAl_2O_4$ particles which act as potential nuclei to refine α-Al grains whilst providing reinforcement to enhance the tensile strengths of the alloy. Experimental results showed that the naturally formed $MgAl_2O_4$ particles in the alloy melt were approximately 1 µm in diameter and are very limited in number as observed in the concentrated samples obtained via filtration. With the implementation of the high shear technology on the alloy melt, it is possible to synthesize a large number of fine $MgAl_2O_4$ particles which were approximately 80 nm to 300 nm in diameter. The yield strength of the alloy containing such in-situ sub-nano-sized particles was found to increase from 147 MPa to 169 MPa in the as-cast state. Following treatment with direct ageing at 155°C only, the yield strength of the alloy treated with high melt shear was found to increase by 128 MPa, ultimately achieving a yield strength and ultimate tensile strength of 297 MPa and 423 MPa respectively. The improvement of the mechanical properties of the alloy is attributed to the fine and uniform microstructure achieved by the enhanced heterogeneous nucleation of both α-Al grains and α-AlFeMnSi intermetallic compound via the in-situ $MgAl_2O_4$ particles, and also to the enhanced precipitation strengthening trigged by the increased dislocation density caused by the in-situ $MgAl_2O_4$ particles.

Keywords: Mechanical property; High pressure die casting; High shearing; Al alloy

Introduction

To reduce CO_2 emissions in both the automotive and the electrolytic Al industry, Al9Si3Cu alloy made by the recycled Al alloys is widely used in automotive applications via the high pressure die casting (HPDC) process to produce components with thin walls and complicated shapes due to its excellent mechanical properties, castability and relatively low cost [1,2]. In terms of its composition, most of these alloys have a high Fe tolerance of up to 1.3wt.% and are usually produced from mixed recycled alloys. For most Al alloys, Fe is considered an impurity because of its tendency to form brittle and coarse secondary phases or sludge and its detrimental effects on the mechanical properties of the casting [3–5]. However, for the utilization of HPDC as a shaping casting approach, alloys containing a certain level of Fe and/or Mn still have their advantages due to the reduced tendency of die soldering and the prolonged lifetime of the die [2-3]. There still exists a contradiction between the use of Fe or Mn to avoid the sticking tendency and eliminating the deterioration of mechanical properties caused by the presence of these elements, achieved by the

necessary morphology modification of the undesired phases. Therefore, a huge challenge arises for further improvement of the mechanical properties of Al9Si3Cu alloy to meet the ongoing light weighting demands of the automotive industry and subsequently contribute to a further reduction of CO_2 emissions.

In terms of the high content of Fe in Al9Si3Cu alloy, Fe bearing phases in this kind of alloys mainly are α-AlFeMnSi phase with a Chinese script or polyhedral morphology and β-AlFeSi phase with a coarse needle morphology. Compared to α-AlFeMnSi, β-AlFeSi phase is more harmful to the tensile strength and ductility due to its coarse size and angular morphology. To decrease the adverse effect of Fe, the traditional approach is to modify the β-AlFeSi phase to α-AlFeMnSi through chemical composition modification [2,6-8], i.e., the addition of elements, such as Mn and/or Cr, into the molten Al alloys prior to solidification.

Recently, Ji et al [9] studied the influence of the Mn/Fe ratio on the transformation of Fe bearing phases from β-AlFeSi to α-AlFeMnSi, and they suggested that a Mn/Fe ratio greater than 0.5 is preferable to favorite the formation of α-AlFeMnSi about 20-50 µm in size and to suppress β-AlFe in Al-Mg-Si alloys. With the addition of 0.02-0.54% Mn, the yield strength of the alloy increased from about 125 MPa to 140 MPa. But the increase of Mn/Fe ratio would result in the increase of number and size of the primary α-AlFeMnSi phases [10]. The area fraction and size of the α-AlFeMnSi intermetallic compound increases as the Cr content increases [2]. During HPDC processing, this kind of the primary intermetallic phase may form in the stage of the melt after being poured into the shot sleeve and before being injected into the die cavity, due to the temperature of the partial melt being lower than the nucleation temperature. This type of primary compound phases will remain in the final component after solidification as one of the microstructure characteristics, giving a detrimental influence on the variability of mechanical properties [9-12]. The primary α-AlFeMnSi phase is usually of coarse size and is commonly referred to as sludge [2,6,8,10,13]. Due to its relatively high specific density, sludge tends to settle down to the bottom of the holding crucible, subsequently altering the chemical composition of the melt and increasing the tendency of die sticking [6]. Narayanan et al [14] studied the crystallization behavior of A319 alloy with different melt superheats and showed that a lower superheat below 750°C would result in the existence of β-AlFeSi phase due to the formation of γ-Al_2O_3 and its function of acting as nuclei for β-AlFeSi phase to nucleation. At a higher melt temperature of more than 850°C, for instance, could lead to the formation of α-Al_2O_3 and subsequently nucleate α-AlFeMnSi phase in the following solidification process. Khalifa et al [15] investigated the performance of oxides, carbides and borides on the formation of Fe-intermetallic phase in Al-Si-Fe alloy by introducing particles into the melt by adopting a gas injection approach. The study revealed that CaO and SiC are potent nucleation sites for α-AlFeMnSi phase. The more effective approaches of further reducing the size of α-AlFeMnSi phase are still under development. Cao and Campbell investigated the planar disregistries between the oxides of the MgO, $MgAl_2O_4$, Al_2O_3 and the α-Fe phase in Al-Si-Mg alloys showing that the oxides might be good substrates for the nucleation of α-Fe [16,17]. Miller et al suggested that the iron-rich intermetallic phases, such as a-$Al_{15}(Fe,Mn)_3Si_2$ and β-Al_5FeSi, can nucleate on oxide films entrained in aluminum casting alloys [5].

As one of the most important strengthening mechanisms, precipitation usually contributes dramatically to an improvement in the mechanical properties of materials. To make full use of precipitation strengthening, appropriate heat treatment procedure is required to: (i) obtain a maximum super-saturated solid solution via the high temperature solution process, (ii) maintain the super-saturated status by quenching and (iii) produce fine scale precipitates by subsequent solution decomposition at low temperature (this stage is referred to as ageing or annealing). A good super-saturated solid solution is a crucial prerequisite to obtain the expected precipitates. According to the solidification process, cooling down from liquid to solid, it is possible to achieve a super-saturated solid solution with rapid solidification at a higher cooling rate, in which the solubility is determined by the alloy composition and the cooling rate. For Al9Si3Cu alloy, Mg, Cu and Si have relatively good solubility in the solid Al matrix and Al_2Cu (θ) and $Al_5Cu_2Mg_8Si_6$ (Q) are the main kinds of precipitates [18].

The HPDC process has a characteristically high cooling rate of about 500-1000K/s, which is not achievable by other casting methods. Therefore, super-saturated α-Al could be achieved under such a high cooling rate and direct ageing can be employed to obtain further precipitation strengthening without suffering from solutionizing and quenching processes. Considering the complex shape and thin wall thickness of the castings produced by HPDC, there is a high risk of torsion deformation for components to suffer if they are subject to solution treatment and quenching into water. Therefore, direct ageing treatment after the HPDC casting, namely precipitation treatment, is one approach to improve the yield strength of the material by utilizing the limited solubility to obtain precipitates. Lumley et al [19] studied the influence of various heat treatment methods on the improvement of properties of A380 alloy. It was reported that with direct ageing at 150 ℃, the yield strength increased by 62 MPa while the elongation decreased by 50% compared to a yield strength of 172 MPa and an elongation of 4% in the as-cast state. After full heat treatment of solution at 490℃ for 15 min followed by quenching in water and ageing at 150℃, the yield strength, ultimate tensile strength and elongation were found to achieve values of 353 MPa, 431 MPa and 3% respectively.

Dislocations were found to promote the nucleation and growth of precipitate during ageing treatment. Gazizov et al [20] studied the effect of pre-straining on the ageing behavior and mechanical properties of an Al-Cu-Mg-Ag alloy. The study demonstrated that dislocation density significantly increased by pre-straining before ageing, affecting the dimension and number density of Ω-phase and θ-phase via nucleation enhancement. It was proved by Yang et al [21] and Feng et al [22] that the precipitation process is mainly along dislocations in Mg-Zn and Al-Cu-Mg alloys. Liu et al [23] studied the growth of precipitates in Al-Cu alloy via in-situ scanning transmission electron microscopy (STEM), in which the growth of a precipitate was found to be strongly enhanced when it coincides with a dislocation.

For cast Al alloys, one of efficient approaches to increase dislocation density is to introduce solid particles into Al matrix as reinforcement and to develop a stress concentration using the difference in thermal expansion coefficient between the particles and Al matrix. For instance, the addition of 2 wt.% SiC particles into Al alloys can increase the dislocation density by 100 times than that of the matrix alloy [24].

To reveal the influence of the highly super-saturated solid solution formed during the HPDC process and the subsequent improvement of dislocation density in Al9Si3Cu alloy, the present study aims to synthesize in-situ $MgAl_2O_4$ particles within the melt to substantially increase the dislocation density in the final component after solidification. Direct ageing treatment is then carried out for the HPDC samples to investigate the key mechanism resulting in further improvement to the mechanical properties of the alloy.

Experimental

LM24 alloy ingots supplied by Norton UK, was employed as the raw material in this study. The alloy mainly consists of 8.09%Si, 3.11%Cu, 1.78%Zn, 0.86%Fe, 0.22%Mn, 0.16%Mg and 0.04%Ti (all in wt.%). Clay-graphite crucible was then used with 10 Kg of the alloy per batch. When the melt temperature reached 725±5ºC, a 1 hour holding time was adopted to obtain the naturally forming $MgAl_2O_4$. The melt was then heated up further to 750ºC for melt purification by rotary degassing technology for 8 min at 350 rpm rotation speed, in which Ar was introduced to the bottom of the rotor with flow rate of 4 L/min. The cleaned melt was then manually poured into the shot sleeve to produce tensile samples of 6.35mm in diameter by a Frech 4500kN locking force cold chamber HPDC machine. The pouring temperature of the melt, die temperature and shot sleeve temperature were 680ºC, 200ºC and 180ºC respectively.

To investigate the influence of $MgAl_2O_4$ particles on the properties of LM24 alloy, another 10Kg of LM24 alloy was melted in another crucible at 725±5ºC and holding for 30 minutes for composition uniformity. The melt conditioning treatment via rotor-stator high shearing unit was employed at a speed of 1500rpm for 30 minutes at 725±5ºC (LM24-M), in order to allow the in-situ $MgAl_2O_4$ particles to form in the melt. After melt conditioning, rotary degassing was used to purify the melt and the same casting parameters were used to obtain the HPDC tensile samples. After stabilization at room temperature for 24 hours, some of the tensile samples underwent ageing at 155±5ºC for 15 hours. Tensile testing was carried out on an Instron 5500 Universal electromechanical testing system at ambient temperature. Ramping rate was 1mm/min and a 50mm extensometer was used to record tensile data.

To analysis $MgAl_2O_4$ particles formed in the alloy melt, melt filtration was used to collect particles in the melt using a prefill machine (Footprinter, ABB Inc.) [25,26]. The molten alloy was poured into a pre-heated crucible at 720±5º C and then was forced to go through a filter located at the bottom of the crucible under a pressure of 0.8 bar. Due to the blocking effect of the filter disc having very fine pore size on the solid phases in liquid melt, the particles with size above tens nanometer will not be forced through the filter and remain on the top of the filter instead [27–29]. After solidification, samples for analysis of the size and morphology of the particles were taken from the top of the filter perpendicular to the filtration direction. Samples for microstructural observation were prepared by a standard procedure, and microstructural analyses were carried out using Zeiss optical microscopy, Zeiss Supra 35VP field-emission scanning electron microscopy (FE-SEM) equipped with an energy dispersive X-ray spectroscopy (EDS) detector, and JEOL-2100 transmission electron microscopy (TEM), respectively.

Results and discussions

Figure 1 shows that the comparison of the tensile properties of LM24 and LM24-M alloys at both the as-cast and aged state. At as-cast state, both the yield strength (YS) and ultimate tensile strength (UTS) of the LM24-M alloy are improved. Compared to the LM24 alloy, the YS of the LM24-M alloy increased from 147±3 MPa to 169±3 MPa and the UTS increased from 339±5 MPa to 355±5 MPa, whilst the elongation remained in a quasi-steady state.
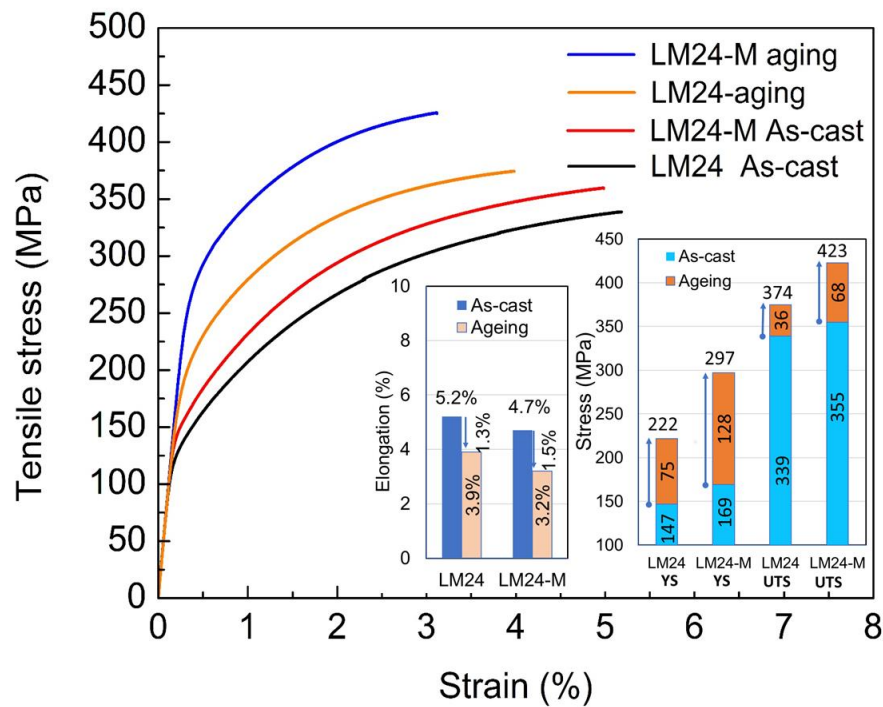

Figure 1 Tensile properties of LM24 and LM24-M alloys at as-cast state and ageing at 155ºC for 15 hours.

After direct ageing, there is a similar trend of the strength improvement for these two kinds of alloys. For LM24 alloy, the YS and UTS increased by 75 MPa and 36 MPa respectively, whilst elongation decreased from 5.2% to 3.9%. With high shearing imposed, the YS and UTS of the LM24-M alloy increased by 128 MPa and 68 MPa respectively, and the elongation decreased from 4.7% to 3.2%. This trend of properties change with heat treatment is in strong agreement with the results of Lumley et al [19]. Considering the mechanism behind the direct ageing process, the improvement in mechanical properties indicates that direct ageing after HPDC casting can promote the precipitation strengthening effect. It should be noted that the improvement of both YS and UTS for the LM24-M alloy is far more substantial than that of the LM24 alloy. After directly ageing, the YS and UTS of the LM24-M alloy is 297±5 MPa and 423±5 MPa, respectively, compared to the YS of 222±3 MPa and UTS of 374±5 MPa of LM24 alloy after the ageing. It has reported that a YS, UTS and elongation of 280 MPa, 380MPa and 4.2% were achieved respectively for an Al9Si3Cu alloy with 0.1%Mg [18], after full heat treatment of solution at 510ºC for 30min and ageing at 170ºC for 24 hours. By considering both results reported previously in the literature and the experimental findings presented in this study, it can be shown that by proper alloy design the mechanical properties of LM24 alloy

with direct ageing only can be improved and can achieve the same level of performance as the alloy after full heat treatment.

Generally, the improvement of YS is determined by grain size and the secondary strengthening phase. The microstructure of the LM24 alloys produced without and with high shearing is shown in Figure 2, with α-Al and α-AlFeMnSi phase being clearly seen. With high shearing, the primary α-Al crystals formed in both the shot sleeve (α-Al$_1$) and the die cavity (α-Al$_2$) are uniform and of a fine grain size. The fine grain structure of the LM24-M alloy illustrates that the application of high shear can enhance the grain refinement of α-Al. From a grain refinement strengthening point of view and considering the Hall-Petch equation, the YS of the material is inversely proportional to the square root of grain size. Therefore, in the present study, grain refinement could be attributed to the improvement in strength.
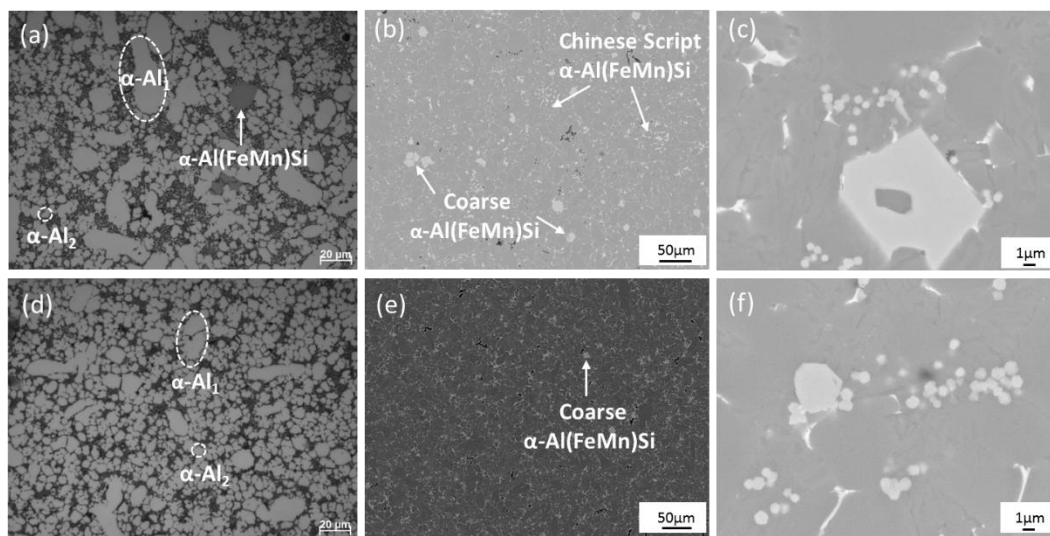

Figure 2 Grain size of LM24 (a) and LM24-M (d) alloy at as-cast state, α-Al$_1$ is formed in shot sleeve and α-Al$_2$ is formed in die cavity. Morphology and size of coarse α-Al(FeMn)Si particles formed in shot sleeve, and fine α-Al(FeMn)Si particles formed in die cavity of LM24 (b, c) and LM24-M (e, f) alloy respectively. Compared to LM24 alloy, LM24-M alloy has fine α-Al grains and uniform microstructure.

Considering the solidification of HPDC LM24 alloys, there are two types of Fe-bearing intermetallics that form during different stages of solidification. Primary α-AlFeMnSi phase forms in the shot sleeve solidification stage, usually having coarse size and Chinese script/polyhedral morphology. Pro-eutectic α-AlFeMnSi phase formed in the die cavity has fine size and polyhedral or hexagonal morphology.

Figures 2b and 2e show the size and morphology of the coarse α-AlFeMnSi phase in LM24 alloys without and with high shearing respectively. Without high shearing, the coarse α-AlFeMnSi phase exhibits a Chinese script and polyhedral morphology. The average size is about 15 μm for the polyhedral α-AlFeMnSi phase and about 50 μm for the Chinese script α-AlFeMnSi phases, as shown in Fig.2b. With high shearing, both the size and quantity of the coarse α-AlFeMnSi phase significantly changes. The Chinese script phase is eliminated and the size of the coarse polyhedral α-AlFeMnSi

phase is reduced to about 10 μm. Furthermore, the amount of polyhedral α-AlFeMnSi phase in the LM24-M alloy (Fig.2e) is much lower than in the LM24 alloy (Fig.2b).

Figures 2c and 2f reveal the morphology of the fine α-AlFeMnSi phase formed in the die cavity of LM24 and LM24-M alloy respectively. The fine α-AlFeMnSi phases in these two alloys have the same hexagonal morphology and similar size of about 1μm in diameter. Compared to LM24 alloy, the fine α-AlFeMnSi particles are slightly larger in size, and many of these fine particles were observed in the LM24-M alloy. In terms of the strengthening mechanism of particle reinforced metal matrix composites, the fine α-AlFeMnSi particles can act as useful reinforcement to enhance the tensile properties, but an adverse effect of these particles is that they will decrease the ductility of the material.

The change of the microstructure of LM24-M alloy indicates that effective nuclei for the refinement of grain size and α-AlFeMnSi phase were formed during high shear melt conditioning. It is very difficult to find and analysis these particles due to their limited number and very fine size in the tensile samples. To observe their size and morphology directly, pressure melt filtration was employed in the present study to collect such particles.

Figure 3 shows the size, morphology and composition of the particles collected from the LM24 and LM24-M alloy melts by the melt filtration. As shown in Fig. 3a, 3b (the composition of the particles can be given by a table), there are two types of particles present in the LM24 alloys melt, TiB_2 and $MgAl_2O_4$ (Spinel). The grey particles with hexagonal morphology are TiB_2, which is approximately 1μm in size. In the present study, no additional AlTiB grain refiner was added during melt treatment. Therefore, the TiB_2 particles were introduced during the production of the LM24 alloy ingots as these ingots are prepared from secondary recycled alloys. Considering the similar amount of TiB_2 particles in LM24 and LM24-M alloys, comparison of the microstructures in Fig. 2 indicate that these types of TiB_2 particles have limited contribution to microstructural refinement during the HPDC process. There should be another mechanism for α-Al grain refinement and α-AlFeMnSi refinement for LM24-M alloy with high shearing.

With natural oxidation, $MgAl_2O_4$ spinel particles usually formed in Mg-containing Al alloys, with their size being about 1 μm and few of such particles are observed, as shown in Fig.3a. After high shearing, the amount of the $MgAl_2O_4$ particles in LM24-M alloy (Fig. 3b) was much greater than in the LM24 alloy. In addition, the size of spinel particles was much smaller than those in the LM24 alloy and a bimodal particle size distribution of approximately 80 nm and 300 nm was observed. This means that melt conditioning by high shear promotes the formation of the $MgAl_2O_4$ particles. It has been previously demonstrated that the spinel particles are the effective nuclei for α-Al in purity Al [30,31] and Al-Mg alloy [32] due to the small lattice misfit of about 1.4% between the spinel and Al along the specific orientation relationship: $(111)[110]_{MgAl2O4}//(111)[110]_{α-Al}$. Our previous study indicated that in Al-9.4Si-2.3Cu-1.0Zn-0.49Mg alloy the $MgAl_2O_4$ particle still is the effective nucleation substrate for α-Al [33]. According to the free growth model [34], the undercooling required for crystal nucleation is inversely proportional to the size of the nuclei. Larger nuclei are the first nucleation sites during solidification. Al-5Ti-1B grain refiner, a commercial master alloy, was widely used in Al industry to refine the

α-Al and to improve the mechanical properties of the materials, in which the TiB_2 particle with a thin layer of $TiAl_3$ on its surface formed in the synthesis process of Al-5Ti-1B refiner was considered as the effective nucleation substrate for α-Al [35–39]. The TiB_2 particle has a distribution range between 200 nm and 6 μm in size, and its average size is about 1μm [34]. In present study, there is a similar amount of TiB_2 particles in LM24 and LM24-M alloys. However, the smaller grain size in LM24-M alloy, as shown in Fig. 2, illustrates that the TiB_2 particles with such kind of size distribution do not have effective refinement performance during the HPDC process. Therefore, the refinement of the α-Al_1 in LM24-M alloy (Fig.2d) indicates that the spinel particles about 300 nm in diameter are the effective nucleation sites during solidification in the shot sleeve. During secondary solidification in the die cavity, the small spinel particles act as the nucleation sites due to the high thermal undercooling caused by the very high cooling rate.
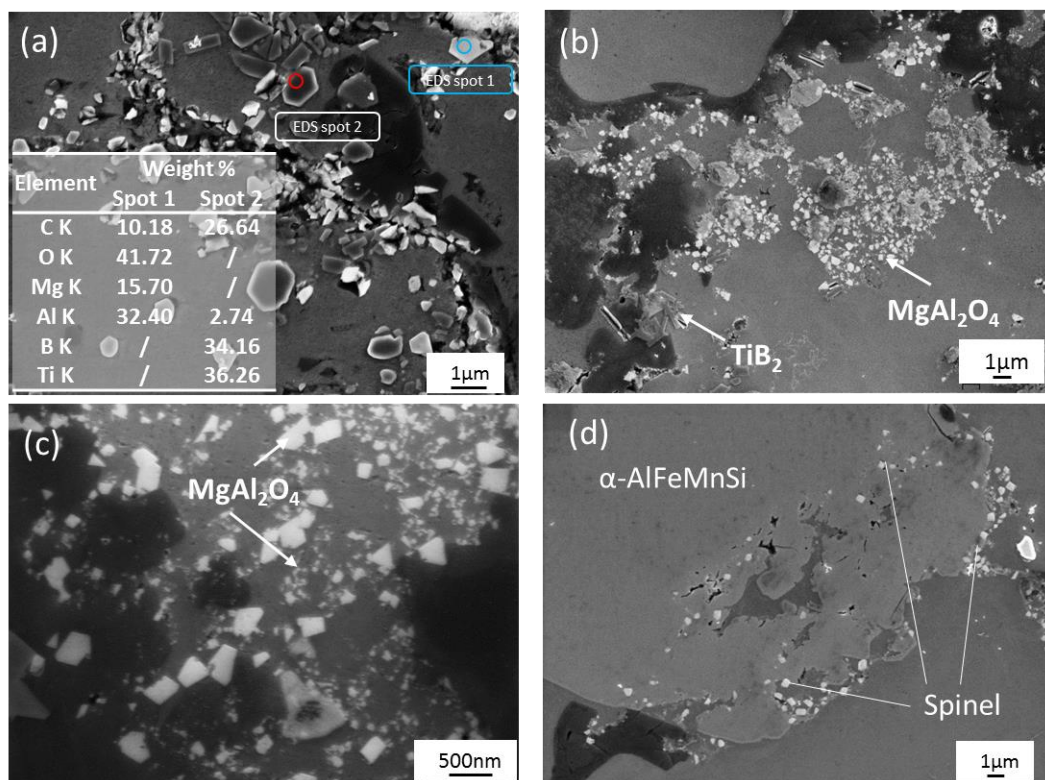

Figure 3 Particles collected from LM24 alloy melt (a) and high shearing LM24-M melt (b) via pressure filtration method, the black particle is TiB_2 and light grey one is $MgAl_2O_4$ according to the compositions in insert table. The main size distribution of $MgAl_2O_4$ particles in LM24-M alloy is about 80nm and 300nm in diameter (c), which is much smaller than that in LM24 alloy. Many spinel particles are observed on the surface of α-AlFeMnSi in LM24-M alloy (d).

The coarse primary α-AlFeMnSi phase forms near to the wall when the melt is transferred into the shot sleeve and will be transported into the die cavity to remain in the final microstructure of the casting. During tensile testing, fracture of the LM24 alloy samples initiates by the cracking of eutectic phases of Si and the coarse α-AlFeMnSi phases due to high tensile stresses induced by plastic deformation in the matrix. Therefore, the intermetallic phases of small size have less harmful influence on the mechanical properties. In the present study, comparison of the microstructures

of LM24 (Fig.2b) and LM24-M alloy (Fig.2e) indicates that high shearing refines the coarse α-AlFeMnSi phase effectively (Fig.2e). To analysis the behavior of spinel particles on the formation of α-AlFeMnSi phase, the microstructure was observed close to the top of the filter, as shown in Fig. 3d. It is noted that many spinel particles are trapped on the surface of the coarse α-AlFeMnSi phase in the LM24-M alloy. Coarse α-AlFeMnSi forms in the filter samples due to the very slow solidification process that occurs after filtration has completed, which can be attributed to the good thermal insulation performance of the crucible used for filtration. The entrapment of spinel particles by the growth of α-AlFeMnSi indirectly proves the orientation relationship and nucleation behavior between spinel and α-AlFeMnSi. Characteristics of the $MgAl_2O_4$ particles observed in the filter samples (Fig. 3c) and the microstructure of LM24-M alloy (Fig. 2e), reveal that the in-situ spinel particles with such size distributions as those formed using the high shear technology can refine coarse α-AlFeMnSi phases in LM24 alloys. This result is in strong agreement with our previous study of coarse α-AlFeMnSi in A380 alloy refined by intensive melt shearing [40], and with the experimental results of Cao and Campbell that the $MgAl_2O_4$ is the good nucleation substrate for α-Fe phase [16-17].

Compared to the properties of LM24 alloy in the as-cast state, the YS and UTS were found to increase by 75 MPa and 36 MPa respectively whilst the elongation decreased by 1.3% after direct ageing. With the application of high shear melt conditioning for the LM24-M alloy melt, an improvement of 128 MPa and 68 MPa was achieved for YS and UTS respectively, whilst the elongation decreased by 1.5%. The trend in property change after direct ageing is in strong agreement with the performance expected from the precipitation strengthening mechanism, i.e. more precipitation, leads to a further improvement in strength and a further decrease in elongation.

According to the phase diagram calculated by Panda software, the equilibrium phases in the LM24 alloy consist of α-AlFeMnSi, β-AlFeSi, Al_2Cu, $Al_5Cu_2Mg_8Si_6$, primary α-Al and eutectic Si and Al. Direct ageing at 155 ± 5° C has no influence on the morphological change of the existing phases as a lower temperature ageing treatment only benefits the generation of precipitates and assists the movement of dislocations. Among all phases in LM24 alloy, possible precipitates include θ-Al_2Cu and $Al_5Cu_2Mg_8Si_6$. Considering similar chemical composition and ageing parameters employed for both LM24 and LM24-M alloys, the level of improvement in tensile strength for these two kinds of alloys indicates that the existence of $MgAl_2O_4$ particles promote the formation of precipitates during direct ageing treatment and results in further enhancement of the YS and the UTS.

Figure 4 is TEM bright field images and corresponding electron diffraction patterns, showing the microstructure of LM24-M alloy at the as-cast and direct aged state. It can be seen from Fig.4a that many dislocations are present in the LM24-M alloy in the as-cast state, whilst no precipitates were detected in the selected area electron diffraction (SAED) pattern shown in Fig.4b. After direct ageing, many precipitates were observed via TEM (Fig.4c) and the diffraction spots corresponding to precipitates was found in SAED as shown in Fig.4d along [001]$_{Al}$ zone direction. The appearance of precipitates illustrates that the mechanical property improvement of LM24 alloys after direct ageing is attributed to precipitation strengthening.
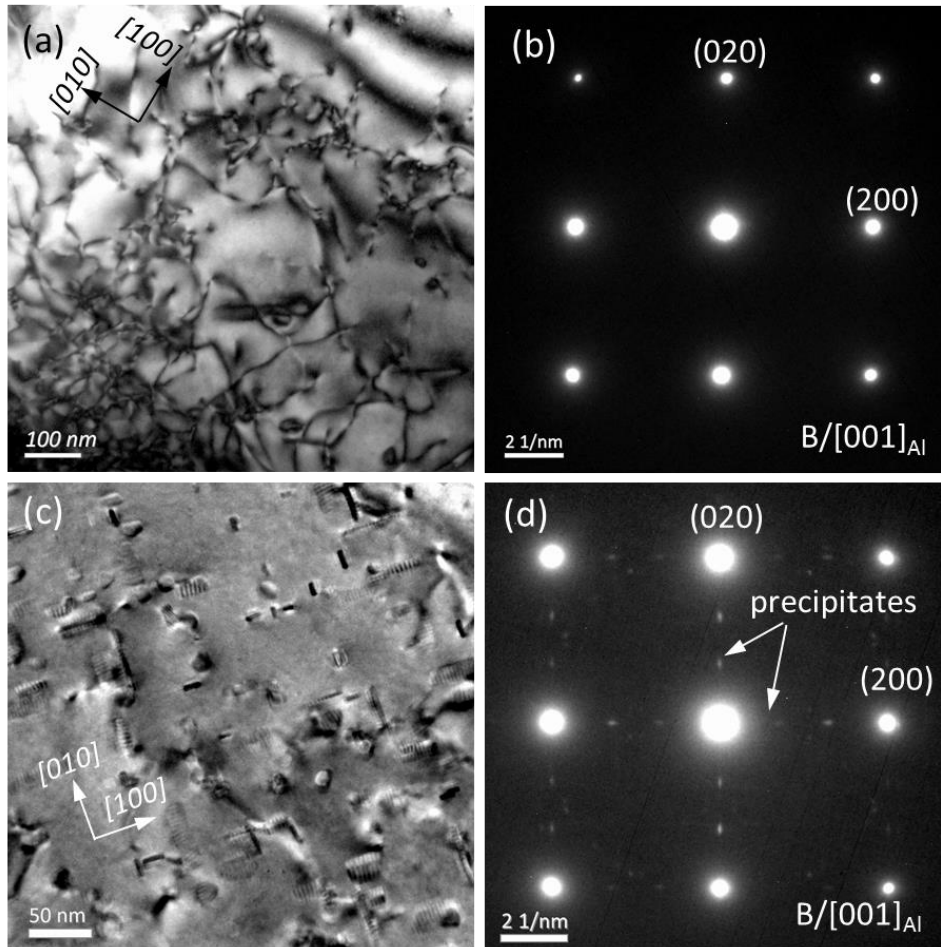
Figure 4 Many dislocations are presented in LM24-M alloy matrix at as-cast state (a) and no precipitates are detected by a selected area electron diffraction (SAED) (b); After direct ageing, lots of precipitates are observed (c) and proved by SAED (d).

Figure 5 reveals further the details of the precipitates in the LM24 alloys after direct ageing. Fig.5a shows the size and morphology of precipitates in the LM24-M alloy. Fig.5b and 5c show the high resolution TEM (HRTEM) image of the Q` phase and the θ` phase, whilst the insert image in Fig. 5b and Fig.5c indicates the fast Fourier transformation (FFT) image of the Q` phase and the θ` phase respectively. Fig.5d shows the Q` phase and θ` phase in LM24 alloy after direct ageing treatment. According to the HRTEM and FFT image in Fig.5 and experiment results of Liu et al [23], the main precipitates in both LM24 and LM24-M alloys are quasi-Q` phase and pre-θ` phase. Compared to the LM24 after full treatment with both solution and ageing treatment having θ` phase as a dominant precipitate [18], in the present study with direct ageing only, the pre-θ` phase and quasi-Q` phase in LM24-M alloy almost

have similar number density. Therefore, both of these two kinds of precipitates contribute to the improvement of tensile strength.

Comparing the size of the precipitates, it can be seen that the length of the θ` phase in both LM24 alloys are very similar at approximately 50 nm. The length of the θ` phase is in strong agreement with Yang`s report of 20-60 nm [18]. But for the length of the Q` phase, there is a significant difference incurred by the condition of the alloy. With full heat treatment, the length of Q` phase is about 20-50 nm [18]. In the present investigation, the Q` phase in LM24 alloy is about 20-40 nm in length and is about 12 nm in length for LM24-M alloy. Considering both the strength improvement observed in the LM24 and LM24-M alloys along with the size and type of the precipitates, the quasi-Q` phase of about 12 nm in length exhibits a far greater enhancement in strength than the larger one.
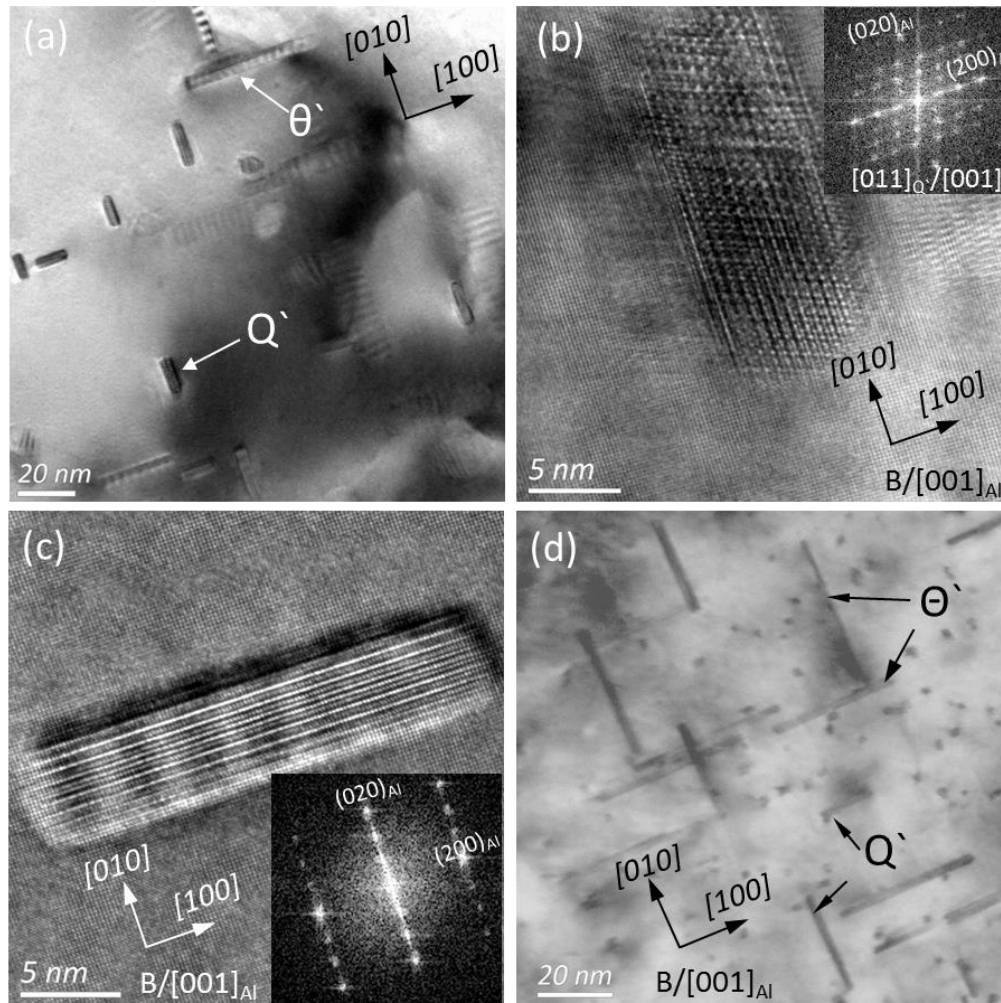
Figure 5 (a) shows the size and morphology of the precipitate phase of θ` and Q` in LM24-M alloy after direct ageing, (b) and (c) show the HRTEM image of the Q` phase and θ `phase, while the insert in figures is the fast Fourier transformation (FFT) image of Q` and θ` respectively. (d) shows the precipitate phase of θ` and Q` in LM24 alloy with direct ageing.

Assuming that the LM24 and LM24-M alloys have the same composition and the only difference between them is that the LM24-M alloy has two kinds of MgAl$_2$O$_4$ particle sizes of about 80 nm and 300 nm in diameter, the alloy can be considered as a particle reinforced Al composite. There are numerous studies having confirmed the formation of dislocations caused by the coefficient of thermal expansion (CTE) in metal matrix composites. The generation of dislocations at the Al/SiC interface has

been observed using a high voltage electron microscope equipped with a double tilt heating stage, and the results suggested that the ceramic particles acted as dislocation sources during cooling from higher temperatures [24]. The relationship between the reinforcement particles and the dislocation density can be described by the equation as follows.

$$\rho = \frac{B\varepsilon V_r}{bd(1 - V_r)}$$

Where B is a geometric constant, ε is the thermal mismatch strain, Vr is the volume fraction of the reinforcement of particles, b is the Burgers vector, and d is the diameter of particles. For given Al alloys, the dislocation density is related to the size and the volume fraction of the particle reinforcement. The greater the volume fraction and the smaller the particles added into the alloy, the greater the dislocation density generated. Basing on the principle relationship between the particles and the dislocation density, the LM24-M alloy in present study has higher dislocation density due to the existence of the of $MgAl_2O_4$ particles produced by the high shearing technology.

The phenomenon of dislocations promoting the nucleation and growth of precipitates has been reported elsewhere [22,23,41]. The precipitation process usually involves two stages: (i) nucleation and growth of precipitates during the early stages and (ii) coarsening of precipitates. During the nucleation and growth of precipitates, dislocations act as the preferred sites for heterogeneous nucleation as the diffusion of vacancies and solute atoms along 'dislocation pipes' is much easier than that in the matrix [31].

It was reported that the θ`-phase particles have {001} habit plane and are nucleated at dislocations with gliding dislocations sweeping the Cu atoms during aging treatment. The increasing dislocation density caused by pre-straining has been shown to affect the dimensions and number density of the Ω-phase particles [20]. Initial precipitation of the Q phase in the matrix has been revealed to occur heterogeneously on dislocations [42]. It has been shown that the growth and coarsening of the platelet η` precipitates are closely correlated to the diffusion of the solute atoms along dislocations. A higher amount of platelet η` forms during the nucleation stage due to the higher density of dislocations providing more sites for heterogeneous nucleation. During the growth and coarsening stage, the depletion of solute atoms caused by the higher number density of the platelet η` formed during nucleation hinders further coarsening of the precipitates and leads to a refinement in the size of the η` precipitates [43]. It was found that, without changing the composition of the alloy, the density of the β` precipitates can increase by applying pre-ageing deformation whilst the length and diameter of the precipitates are reduced. The increasing volume fraction of precipitates and the refinement in the size of precipitates leads to a substantial increase in tensile strength.

According to the related researchers, the main features of the heterogeneous precipitation on dislocations can be summarized as follow: (i) nucleation promotion: dislocations provide the driving force for the nucleation of precipitates and act as preferred sites for heterogeneous nucleation, (ii) growth acceleration and coarsening: dislocations are the fastest path for the diffusion and migration of the solute atoms and

the motion of solute atoms results in the formation of solute enriched regions on dislocations and accelerates the growth of precipitates [44–47].

The improvement in tensile strength of LM24 alloys indicates that the role of dislocations is a critical factor affecting precipitation behavior during direct ageing. Therefore, utilizing dislocations to promote the formation of precipitates is a promising approach to improve the mechanical properties of HPDC alloys, presenting an opportunity for novel alloy design to take advantage of the direct ageing phenomenon.

Conclusions

High shear melt conditioning process is demonstrated to promote the formation of in-situ $MgAl_2O_4$ particles, resulting in an improvement in mechanical properties of the high pressure die cast Al9Si3Cu (LM24) alloy. In comparison to the same alloy without high shearing, the yield strength of the alloy containing in-situ particles increases from 147 MPa to 169 MPa in the as-cast state. This improvement is attributed to the refinement of α-AlFeMnSi phase and the grain refinement of α-Al formed in both the shot sleeve and die cavity. After direct ageing only, the yield strength and ultimate tensile strength of the LM24 alloy treated with high shear melt conditioning rise to 297 MPa and 423 MPa respectively, whilst the elongation decreased to 3.2%, without much sacrifice of the ductility. This significant improvement in tensile strength is attributed to enhanced precipitation strengthening, in which the formation of precipitates is accelerated by a higher dislocation density caused by the presence of in-situ $MgAl_2O_4$ particles.

Data availability

The raw data required to reproduce these findings are available to download from [http://dx.doi.org/10.17632/yt5c9py894.2].

References

[1]   A. Fabrizi, S. Ferraro, G. Timelli, The influence of Sr, Mg and Cu addition on the microstructural properties of a secondary AlSi9Cu3(Fe) die casting alloy, Mater. Charact. 85 (2013) 13–25. doi:10.1016/j.matchar.2013.08.012.

[2]   G. Timelli, F. Bonollo, The influence of Cr content on the microstructure and mechanical properties of AlSi9Cu3(Fe) die-casting alloys, Mater. Sci. Eng. A. 528 (2010) 273–282. doi:10.1016/j.msea.2010.08.079.

[3]   S. Ferraro, A. Fabrizi, G. Timelli, Evolution of sludge particles in secondary die-cast aluminum alloys as function of Fe, Mn and Cr contents, Mater. Chem.

Phys. 153 (2015) 168–179. doi:10.1016/j.matchemphys.2014.12.050.

[4]   S.G. Shabestari, M. Keshavarz, M.M. Hejazi, Effect of strontium on the kinetics of formation and segregation of intermetallic compounds in A380 aluminum alloy, J. Alloys Compd. 477 (2009) 892–899. doi:10.1016/j.jallcom.2008.11.037.

[5]   D.N. Miller, L. Lu, A.K. Dahle, The role of oxides in the formation of primary iron intermetallics in an Al-11.6Si-0.37Mg alloy, Metall. Mater. Trans. B. 37 (2006) 873–878. doi:10.1007/BF02735008.

[6]   S. Ferraro, A. Fabrizi, G. Timelli, Evolution of sludge particles in secondary die-cast aluminum alloys as function of Fe, Mn and Cr contents, Mater. Chem. Phys. 153 (2015) 168–179. doi:10.1016/j.matchemphys.2014.12.050.

[7]   G. Timelli, A. Fabrizi, S. Capuzzi, F. Bonollo, S. Ferraro, The role of Cr additions and Fe-rich compounds on microstructural features and impact toughness of AlSi9Cu3(Fe) diecasting alloys, Mater. Sci. Eng. A. 603 (2014) 58–68. doi:10.1016/j.msea.2014.02.071.

[8]   M. Mahta, M. Emamy, A. Daman, A. Keyvani, J. Campbell, Precipitation of Fe rich intermetallics in Cr- and Co-modified A413 alloy, Int. J. Cast Met. Res. 18 (2005) 73–79. doi:10.1179/136404605225022928.

[9]   S. Ji, W. Yang, F. Gao, D. Watson, Z. Fan, Effect of iron on the microstructure and mechanical property of Al-Mg-Si-Mn and Al-Mg-Si diecast alloys, Mater. Sci. Eng. A. 564 (2013) 130–139. doi:10.1016/j.msea.2012.11.095.

[10]   X. Cao, N. Saunders, J. Campbell, Effect of iron and manganese contents on convection-free precipitation and sedimentation of primary α-Al(FeMn)Si phase in liquid Al-11.5Si-0.4Mg alloy, J. Mater. Sci. 39 (2004) 2303–2314. doi:10.1023/B:JMSC.0000019991.70334.5f.

[11]   A.M.A. Mohamed, A.M. Samuel, F.H. Samuel, H.W. Doty, Influence of additives on the microstructure and tensile properties of near-eutectic Al-10.8%Si cast alloy, Mater. Des. 30 (2009) 3943–3957. doi:10.1016/j.matdes.2009.05.042.

[12]   S. Seifeddine, I.L. Svensson, The influence of Fe and Mn content and cooling rate on the microstructure and mechanical properties of A380-die casting alloys, Metall. Sci. Technol. 27 (2009) 11–20.

[13]   S.G. Shabestari, The effect of iron and manganese on the formation of intermetallic compounds in aluminum-silicon alloys, Mater. Sci. Eng. A. 383 (2004) 289–298. doi:10.1016/j.msea.2004.06.022.

[14]   L.A. Narayanan, F.H. Samuel, J.E. Gruzleski, Crystallization behavior of iron-containing intermetallic compounds in 319 aluminium alloy, Met. Mat. Trans. A. 25 (1994) 1761–1773. doi:10.1007/BF02668540.

[15]   W. Khalifa, F.H. Samuel, J.E. Gruzleski, H.W. Doty, S. Valtierra, Nucleation of Fe-intermetallic phases in the Al-Si-Fe alloys, Metall. Mater. Trans. A. 36 (2005) 1017–1032. doi:10.1007/s11661-005-0295-9.

[16]   X. Cao, J. Campbell, The nucleation of Fe-rich phases on oxide films in Al-11.5Si-0.4Mg cast alloys, Metall. Mater. Trans. A Phys. Metall. Mater. Sci. 34 A (2003) 1409–1420. doi:10.1007/s11661-003-0253-3.

[17]   X. Cao, J. Campbell, Effect of melt superheating on convection-free precipitation and sedimentation of primary α-Fe phase in liquid al-11.5Si-0.4Mg alloy, Int. J. Cast Met. Res. 15 (2003) 595–608. doi:10.1080/13640461.2003.11819546.

[18]   H. Yang, S. Ji, W. Yang, Y. Wang, Z. Fan, Effect of Mg level on the microstructure and mechanical properties of die-cast Al-Si-Cu alloys, Mater.

Sci. Eng. A. 642 (2015) 340–350. doi:10.1016/j.msea.2015.07.008.

[19] R.N. Lumley, R.G. Odonnell, D.R. Gunasegaram, M. Givord, Heat treatment of high-pressure die castings, Metall. Mater. Trans. A. 38 (2007) 2564–2574. doi:10.1007/s11661-007-9285-4.

[20] M. Gazizov, R. Kaibyshev, Effect of Pre-straining on the aging behvior and mechanical properties of an Al-Cu-Mg-Ag alloy, Mater. Sci. 625 (2015) 119–130. doi:10.1016/j.msea.2012.12.042.

[21] Z. Yang, L. Zhang, M.F. Chisholm, X. Zhou, H. Ye, S.J. Pennycook, Precipitation of binary quasicrystals along dislocations, Nat. Commun. 9 (2018) 1–7. doi:10.1038/s41467-018-03250-8.

[22] Z. Feng, Y. Yang, B. Huang, M. Han, X. Luo, J. Ru, Precipitation process along dislocations in Al-Cu-Mg alloy during artificial aging, Mater. Sci. Eng. A. 528 (2010) 706–714. doi:10.1016/j.msea.2010.09.069.

[23] C. Liu, S.K. Malladi, Q. Xu, J. Chen, F.D. Tichelaar, X. Zhuge, H.W. Zandbergen, In-situ STEM imaging of growth and phase change of individual CuAlX precipitates in Al alloy, Sci. Rep. 7 (2017) 1–8. doi:10.1038/s41598-017-02081-9.

[24] M. Vogelsang, R.J. Arsenault, R.M. Fisher, Anin situ HVEM study of dislocation generation at Al/SiC interfaces in metal matrix composites, Metall. Trans. A. 17 (1986) 379–389. doi:10.1007/BF02643944.

[25] X. Cao, Pressure filtration tests of liquid Al − Si cast alloys II . Best-fitted equations for filtrate weight versus filtration time curves, Mater. Sci. Eng. A. 403 (2005) 94–100. doi:10.1016/j.msea.2005.04.038.

[26] G. Yeom, H.K. Lim, S.K. Kim, S. Hyun, Y. Yoon, Effects of Mg Enhancement and Heat Treatment on Microstructures and Tensile Properties of Al2Ca-Added ADC12 Die Casting Alloys, J. Mater. Sci. Technol. 32 (2016) 1043–1048. doi:10.1016/j.jmst.2016.07.015.

[27] Z. Fan, Y. Wang, M. Xia, S. Arumuganathar, Enhanced heterogeneous nucleation in AZ91D alloy by intensive melt shearing, Acta Mater. 57 (2009) 4891–4901. doi:10.1016/j.actamat.2009.06.052.

[28] Y. Zhang, J.B. Patel, Y. Wang, Z. Fan, Variation improvement of mechanical properties of Mg-9Al-1Zn alloy with melt conditioned high pressure die casting, Mater. Charact. 144 (2018) 498–504. doi:10.1016/j.matchar.2018.08.007.

[29] Y. Zhang, J.B. Patel, J. Lazaro-Nebreda, Z. Fan, Improved Defect Control and Mechanical Property Variation in High-Pressure Die Casting of A380 Alloy by High Shear Melt Conditioning, JOM. 70 (2018) 2726–2730. doi:10.1007/s11837-018-3005-y.

[30] D. Zhang, L. Wang, M. Xia, N. Hari Babu, J.G. Li, Misfit paradox on nucleation potency of MgO and MgAl2O4 for Al, Mater. Charact. 119 (2016) 92–98. doi:10.1016/j.matchar.2016.07.018.

[31] L. Yang, M. Xia, N.H. Babu, J. Li, Formation of $MgAl_2O_4$ at Al/MgO Interface, Mater. Trans. 56 (2015) 277–280. doi:10.2320/matertrans.M2014345.

[32] H.T. Li, Y. Wang, Z. Fan, Mechanisms of enhanced heterogeneous nucleation during solidification in binary Al-Mg alloys, Acta Mater. 60 (2012) 1528–1537. doi:10.1016/j.actamat.2011.11.044.

[33] Y. Wang, H.T. Li, Z. Fan, Oxidation of aluminium alloy melts and inoculation by oxide particles, Trans. Indian Inst. Met. 65 (2012) 653–661. doi:10.1007/s12666-012-0194-x.

[34] A.L. Greer, A.M. Bunn, A. Tronche, P. V. Evans, D.J. Bristow, Modelling of inoculation of metallic melts: application to grain refinement of aluminium by

Al-Ti-B, Acta Mater. 48 (2000) 2823–2835. doi:10.1016/S1359-6454(00)00094-X.

[35] D.G. McCartney, Grain refining of aluminum and its alloys using inoculants, Int. Mater. Rev. 34 (1989) 247–260.

[36] B.S. Murty, S.A.Kori, M. Chakraborty, Grain refinement of aluminum and its alloys by heterogenous nucleation and alloying, Int. Mater. Rev. 47 (2002) 3–29.

[37] T.E. Quested, Understanding mechanisms of grain refinement of aluminium aloys by inoculation, Mater. Sci. Technol. 20 (2004) 1357–1369.

[38] M.A. Easton, D.H. StJohn, Grain refinement of aluminum alloys Part I. The nucleant and solute paradigms-a review of the literature, Metall. Mater. Transanctions A. 30 (1999) 1613–1623.

[39] Z. Fan, Y. Wang, Y. Zhang, T. Qin, X.R. Zhou, G.E. Thompson, T. Pennycook, T. Hashimoto, Grain refining mechanism in the Al/Al-Ti-B system, Acta Mater. 84 (2015) 290–304. doi:10.1016/j.actamat.2014.10.055.

[40] H.T. Li, S. Ji, Y. Wang, M. Xia, Z. Fan, Effect of intensive melt shearing on the formation of Fe-containing intermetallics in LM24 Al-alloy, IOP Conf. Ser. Mater. Sci. Eng. 27 (2011) 1–7. doi:10.1088/1757-899X/27/1/012075.

[41] B. Yang, Y.T. Zhou, D. Chen, Local decomposition induced by dislocation motions inside precipitates in an Al-alloy, Sci. Rep. 3 (2013) 1–6. doi:10.1038/srep01039.

[42] G.C. Weatherly, A. Perovic, D.D. Perovic, N.K. Mukhopadhyay, D.J. Lloyd, The precipitation of the Q phase in an AA6111 alloy, Metall. Mater. Trans. A. 32 (2001) 213–218. doi:10.1007/s11661-001-0251-2.

[43] K. Ma, T. Hu, H. Yang, T. Topping, A. Yousefiani, E.J. Lavernia, J.M. Schoenung, Coupling of dislocations and precipitates: Impact on the mechanical behavior of ultrafine grained Al-Zn-Mg alloys, Acta Mater. 103 (2016) 153–164. doi:10.1016/j.actamat.2015.09.017.

[44] L. Ding, Z. Jia, Z. Zhang, R.E. Sanders, Q. Liu, G. Yang, The natural aging and precipitation hardening behaviour of Al-Mg-Si-Cu alloys with different Mg/Si ratios and Cu additions, Mater. Sci. Eng. A. 627 (2015) 119–126. doi:10.1016/j.msea.2014.12.086.

[45] M. Legros, G. Dehm, E. Arzt, T.J. Balk, Observation of giant diffusivity along dislocation cores, Sci. 319 (2008) 1646–1649.

[46] T. Hu, K. Ma, T.D. Topping, J.M. Schoenung, E.J. Lavernia, Precipitation phenomena in an ultrafine-grained Al alloy, Acta Mater. 61 (2013) 2163–2178. doi:10.1016/j.actamat.2012.12.037.

[47] A. Deschamps, F. Livet, Y. Bréchet, Influence of predeformation on ageing in an Al-Zn-Mg alloy-I. Microstructure evolution and mechanical properties, Acta Mater. 47 (1998) 281–292. doi:10.1016/S1359-6454(98)00293-6.